Potential of nanofiltration and reverse osmosis processes for the recovery of high-concentrated furfural streams

Nurabiyiah Mohamad [a], Mònica Reig [b], Xanel Vecino [b], Kelly Yong [a], José Luis Cortina [b,c*]

[a]University of Kuala Lumpur, Malaysian Institute of Chemical and Bioengineering Technology (UniKL MICET), Lot 1988 Kawasan Perindustrian Bandar Vendor, Taboh Naning, Alor Gajah, Melaka, 78000, Malasya.

[b]Chemical Engineering Department, Universitat Politècnica de Catalunya (UPC)-Barcelona TECH; Barcelona Research Center for Multiscale Science and Engineering, C/ Eduard Maristany 10-14, Campus Diagonal-Besòs, 08930 Barcelona, Spain.

[c]CETAQUA, Carretera d'Esplugues, 75, 08940 Cornellà de Llobregat, Spain

*Corresponding author: jose.luis.cortina@upc.edu

ABSTRACT

BACKGROUND:

Furfural is an interesting compound that can be produced from renewable and sustainable resources and it is used in the platform chemicals for the synthesis of biofuels and other chemicals. However, a recovery step is required to separate furfural from lignocellulosic hydrolysates when cellulose-based raw materials are used. In this work, nanofiltration (NF) and reverse osmosis (RO) processes have been evaluated to purify or concentrate synthetic furfural solutions.

RESULTS:

Two NF membranes (NF90 and NF270) and three RO membranes (XLE, BW30, SW30) were evaluated to recover furfural from high-concentrated solutions, containing 9 g furfural/L. Rejection percentages and permeate flux performances were determined, and membranes were characterized by XPS and SEM. Results indicated that higher trans-membrane flux could be obtained by NF membranes, being the highest when using NF membrane (260 ± 14 L/m^2·h) and the lowest with the BW30 membrane (3.3 ± 0.7 L/m^2·h) working at 20 bar. On the other hand, NF270 allowed the passage of furfural (around $84\pm3\%$), while the other tested membranes (NF90, XLE, SW30 and BW30) rejected it (between $67\pm2\%$ and $90\pm3\%$).

CONCLUSION:

For this reason, it can be concluded that NF270 will be an option for furfural purification, while NF90 and RO membranes could be used for concentration purposes.

1. INTRODUCTION

Due to the world population growth, more additional energy and valuable chemicals are needed to replace the commercialized ones, which derived from fossil fuels. In fact, effect of global warming due to the massive burning of fossil fuels, increased the greenhouse gas emissions, price instability, petroleum supply and its scarcity as well as depletion of petroleum [1,2]. The efforts to seek alternative processes with renewable and sustainable feedstock for energy, fuels and chemical resources are indeed crucial. Platform chemicals are an important starting material and act as a building block for derivation of other types of commercialize chemicals. For instance, furfural (furan-2-carbaldehyde) is a versatile furan platform compound, which consists of a hetero-aromatic furan ring and an aldehyde functional group [3]. Furfural is produced from the polysaccharide fraction (hemicelluloses), which is the most abundant fraction in nature from lignocellulosic residues [2,4–7]. Generally, there are two processes taking place in furfural production involving depolymerisation and dehydration [8,9]. Furfural is industrially produced from lignocellulosic biomass of oat hulls, pioneer by Quaker Oat Company (1921) by using sulfuric acid and high-pressurized water as a reaction medium [10,11].

In recent years, furfural has gained a great attention from researchers and bio-industries as its increasing demand is expected due to the broad usage of this versatile chemical in many industries [12–15]. Furfural can be used as a feedstock for 2-methylfuran [16], 2-methylhydrofuran [17], ϒ-valerolactone [18,19], furfuryl alcohol [20], carboxylic acid [21], tetrahydrofurfuryl alcohol [22] and long chain hydrocarbons [23,24] during the production of potential biofuels and fuel additives.

However, the challenge is to produce furfural in an efficiently, economically and environmental friendly way. In this sense, subcritical technology with the utilization of

alcohol solvents gained interest [25,26], since critical conditions of alcohol solvents are considerably lower than ones used with water or other solvents, thereby offering milder condition reactions. For example, new approaches had been studied involving the utilization of ethanol as a main solvent under subcritical conditions (solvolysis reaction) in furfural production from oil palm fronds [27]. However, it is believed that is vital to seek for a better recovery process to separate the furfural from these solvents and increase the furfural purity as an end-product.

Separation methods with membrane processes technology has attracted great attention due to their unique ability to separate and purify process streams [28–33]. Several studies have been intensively investigating the removal, recovery and purification of inhibitors, like furfural, from biomass by using membrane process technology [34–41]. For instance, Sagehashi et al. used a reverse osmosis (RO) membrane (NTR-759HR) to separate phenols and furfurals from pyrolysis of biomass with superheated steam aqueous solution and they observed that furfural was recovered (maximum 70%) by the RO membrane [40].

Although membrane processes technology has a wide usage in purification of inhibitors from biomass hydrolysates, the membrane performance depends on several conditions, such feed concentration, operational parameters and membrane technology itself. In this work it is proposed to utilize several NF and RO membranes for the recovery of furfural due to the fact that the separation of uncharged compounds in RO and NF membranes is based on differences in its membrane properties (e.g. molecular sizes, diffusivities, and solubilities) as they contain dense polymeric layers with no well-defined pores [28]. Therefore, the objective of this study is to investigate the feasibility of recovering high-concentrated furfural from a synthetic solution (furfural-ethanol/water). The feed solution mimicked oil palm biomass hydrolysates, treated by a solvolysis subcritical

process. Then, this solution was treated by NF and RO membranes changing the trans-membrane pressure. Moreover, membrane characterization before and after recovery process was conducted by means of X-ray photoelectron spectroscopy (XPS) and scanning electron microscope (SEM).

2. MATERIALS AND METHODS

2.1. Furfural solution

Furfural ($C_5H_4O_2$, 99%), purchased from Sigma Aldrich (USA) and ethanol absolute (C_2H_6O), supplied from Panreac Quimica (Spain) were used to prepare a synthetic furfural solution (9 g/L), mimicking oil palm hydrolysate stream treated by a solvolysis subcritical process [27]. Furfural was mixed in ethanol/water-based solution with a ratio of 1:99 (v/v). 27 L of the solution were prepared in order to carry out the NF and RO experiments with the lab-scale set-up. The pH of furfural solution was 3.7±0.2.

2.2. Experimental set-up

The experimental set-up used for NF/RO membrane testing with synthetic furfural solution is described elsewhere [42,43]. Furfural feed solution was placed in a 30 L thermostatic tank, which kept a constant temperature (25±2 ºC) during the operational time. This solution was pumped into a test cell (GE SEPA^{TM} CF II) equipped with a NF or RO membrane (0.014 m^2 active membrane area) working in a cross-flow mode (0.7 m/s). During the experiments, several parameters, such as pressure, flow, conductivity, pH and temperature were monitored. After the membrane process, two main streams were obtained: permeate and concentrate, which were recirculated into the feed tank in order to keep a constant concentration.

Tested membranes were supplied by Dow Chemical Company and they consisted of two nanofiltration membrane (NF270 and NF90) and three reverse osmosis membrane

(XLE, BW30, and SW30). The membrane characteristics for all five membranes are shown in **Table 1**.

Table 1. Characteristics of membranes tested.

MEMBRANE	NF270[a]	NF90[b]	XLE[c]	BW30[d]	SW30[e]
Membrane type[f]	Semi-aromatic TFC*	Fully aromatic TFC			
		Uncoated		Coated	
pH range (25 °C)	2-11				
Max. temperature (°C)	45				
Max. pressure (bar)	41				69
Max. pressure drop (bar)	0.9			1	

a 44, b 45, c 46, d 47, e 48, f 49; *TFC= Thin Film composite (TFC).

It can be seen in Table 1 three uncoated membranes (NF270, NF90 and XLE) and two coated membranes (BW30 and SW30) were tested. Regarding the data sheet of each membrane, all of them work properly at the pH (3.7±0.2), temperature (25±2 °C) and pressure range (maximum 22 bar) studied.

2.3. NF and RO experimental procedure

Before starting the experimental tests, a cleaning procedure was done to the membrane in order to (i) remove conservation products and (ii) test the membrane steadiness. For this reason, each membrane was soaked into Milli-Q water overnight before being placed into the cell-test. Then, deionized water was circulated through the membrane during 2 hours at maximum trans-membrane pressure (TMP) and maximum velocity cross-flow (vcf), being 22 bar and 1 m/s, respectively. Once the pre-cleaning procedure was done, the furfural solution was placed into the feed tank in order to start the

experiments taking an initial feed sample. In each experiment vcf was kept constant at 0.7 m/s, whereas TMP was increased (2 by 2 bar) from the osmotic pressure to 20 bar. Permeate samples were collected in order to measure the furfural concentration at each operational TMP. Lastly, a final sample was removed from the feed tank to check the furfural concentration evolution. After each experiment, the system was rinsed with deionized water until the water flux and permeability were restored. Then, it was possible to proceed with the next filtration process using a different type of membrane. All of the assays were carried out in duplicate for each membrane tested.

2.4. Operational parameters

The TMP was calculated taking into account the system pressures around the membrane stack, as follows (**Equation 1**):

$$TMP\ (bar) = \frac{P_F + P_C}{2} - P_P \tag{1}$$

where P_F is the feed pressure entering into the cell-test (bar), P_C is the outgoing pressure in the concentrate stream (bar) and P_P is the outgoing pressure in the permeate stream (bar).

During the experimental test, trans-membrane flux (Jv) was also calculated by **Equation 2**:

$$Jv\ \left(\frac{L}{m^2 \cdot h}\right) = \frac{Q_P}{A} \tag{2}$$

where Q_p is the permeate flow (L/h) and A is the active membrane area ($0.014\ m^2$).

Moreover, **Equation 3** was used to determine the obtained rejection (R) percentage when using different NF and RO membranes:

$$R\ (\%) = \frac{C_F - C_P}{C_F}\ x\ 100 \qquad (3)$$

where C_F is the furfural concentration in the feed solution (mg/L) and C_p is the furfural concentration in the permeate stream (mg/L).

2.5. Analytical methodologies

Ultraviolet-visible spectroscopy (UV-Vis) was used as analytical technique to determine the furfural concentration in each sample. Identification of furfural compound in the samples was carried out by measuring the sample absorbance at wavelength of 277 nm and based on furfural standard calibration curves [50,51].

2.6. Membrane characterization

The elementary composition of membrane active layer, before and after furfural recovery, was analysed by an XPS (SPECS system, Germany) using a XR-50 dual anode (Mg/Al) source operating at 200 W and a Phoibos 150 detector (MCD-9). The area of analysis was 3.75 mm^2 and accuracy of binding energies was 284.8eV.

Moreover, morphology SEM images of NF and RO membranes, before and after filtration processes, were obtained using a Jeol JSM-7001F scanning electron microscope, operating at an acceleration voltage of 2.0 keV for secondary-electron imaging (SEI) and x2000 magnifications.

Prior to XPS and SEM analysis, membrane samples were completely dried under vacuum at 40 °C for 24 h.

3. RESULTS AND DISCUSSION

3.1. Trans-membrane flux evolution

Solutions containing 9 g/L of furfural in ethanol/water were driven towards NF and RO membranes from osmotic pressure until 20 bar at pH 3.7±0.2. **Figure 1** shows the trans-

membrane flux (Jv) as a function of TMP for NF (**Figure 1a**) and RO (**Figure 1b**) membranes, respectively.
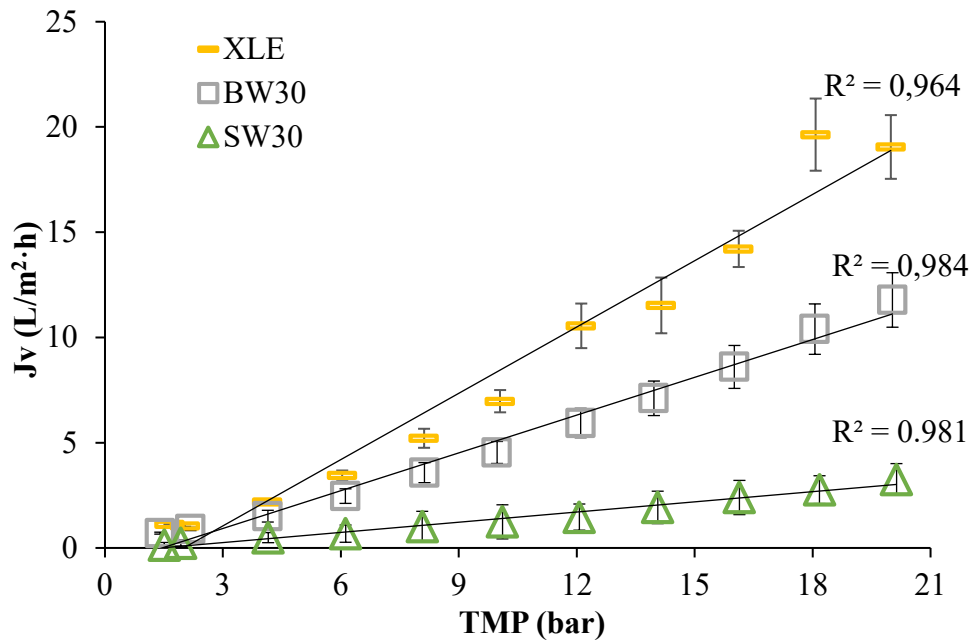
a)
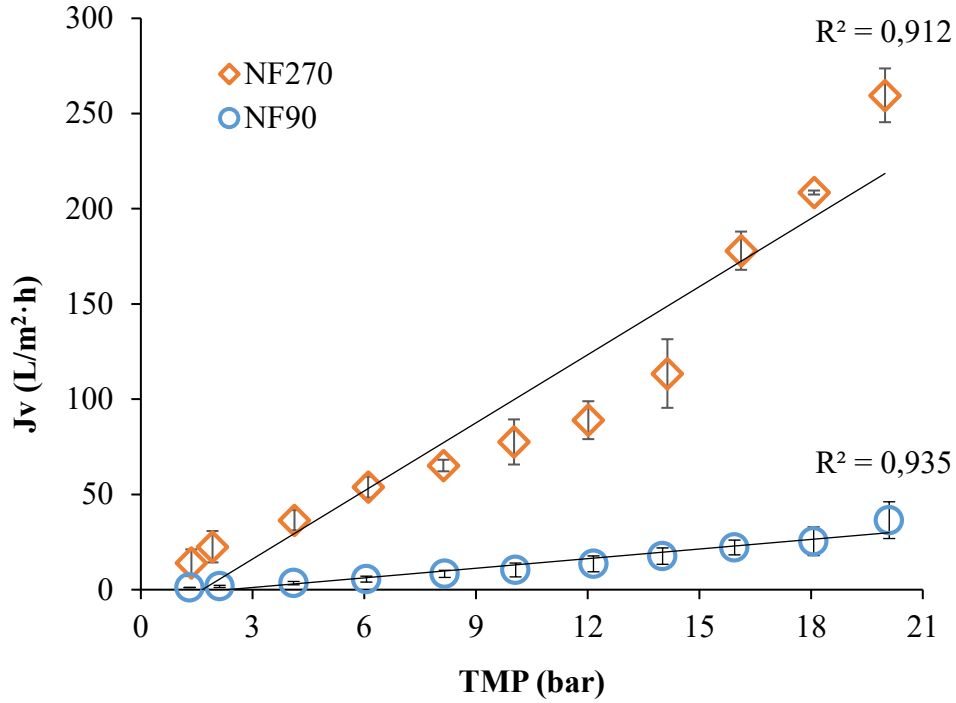
b)

Figure 1. Trans-membrane pressure evolution with the trans-membrane flux for a) NF (NF270 and NF90) and b) RO (XLE, BW30, SW30) membranes, respectively.

It can be seen that as the TMP value increased, Jv obtained also increased. Therefore, higher Jv values allowed to obtain higher flow of permeate. The highest trans-membrane flux values were achieved using NF membranes, being 260±14 L/m²·h and 37±10 L/m²·h using NF270 and NF90 membranes, respectively, when working at 20 bar. On the other hand, the RO membranes, e.g. XLE and BW30, showed similar Jv values (19±2 L/m²·h and 12±1 L/m²·h respectively), while SW30 offered the smallest Jv value (3.3±0.7 L/m²·h) at 20 bar. The higher trans-membrane flux when using the NF membranes, in comparison when employing RO membranes, could be explained because the molecular weight cut-off (MWCO) of each membrane. NF270 has the highest MWCO of 400 Da, followed by the NF90 membrane (MWCO 200 Da) [52] and finally the RO membranes, which all of them have a MWCO of 100 Da [53–55].

Since NF270 is the most studied membrane in the literature, it can be compared easily with the already reported works. Then, fixing the operational conditionals as follows: (i) TMP of 11 bar, (ii) pH=3 and (iii) with NF270 membrane, Dos Santos et al. [38] achieved a trans-membrane flux value of 46 L/m²·h for olive stones auto-hydrolysis liquors containing 2.5 g/L of furfural. Qi et al. [34] showed a Jv value of 53 L/m²·h treating 4 g furfural/L, whereas in this work, the Jv value achieved was 83 L/m²·h using 9 g/L of furfural solution. Thus, comparing these works, it could be appreciated that higher concentration of furfural involves higher trans-membrane flux value, when working at a fixed TMP, pH and membrane.

On the other hand, Qi et al. [34] postulated that fouling could occur due to permeate flux variations, which can also produce fluctuations on the element retention. They observed that membrane fouling and compaction effects were negligible in the pressure range

studied (5-22 bar), because of the linearity of permeate flux and TMP. Thus, to corroborate the linearity of the trans-membrane flux and TMP curves obtained in this work, trend lines were added to **Figure 1**. Jv-TMP linearity was confirmed since the regression coefficients for all curves were higher than 0.900, being the ones for NF membranes (**Figure 1a**) lower (0.912 and 0.935 for NF270 and NF90, respectively) than the ones obtained by RO membranes (from 0.964 to 0.984) (**Figure 1b**). As can be seen in **Figure 1a**, the linear model for NF270 does not fit properly with the last three points (TMP applied from 16 to 20 bar), thus the lowest regression coefficient was obtained for the NF270 membrane. Then, some fouling effects could be expected in this membrane, which have been studied by membrane characterization techniques.

3.2. Furfural rejection evolution

Figure 2 shows the furfural rejection percentage by using NF and RO membranes as function of the trans-membrane flux (Jv), applying TMP from osmotic pressure to 20 bar. According to the solution-diffusion model, it is noted that rejections increase with trans-membrane flux until a constant plateau is reached [39,42].
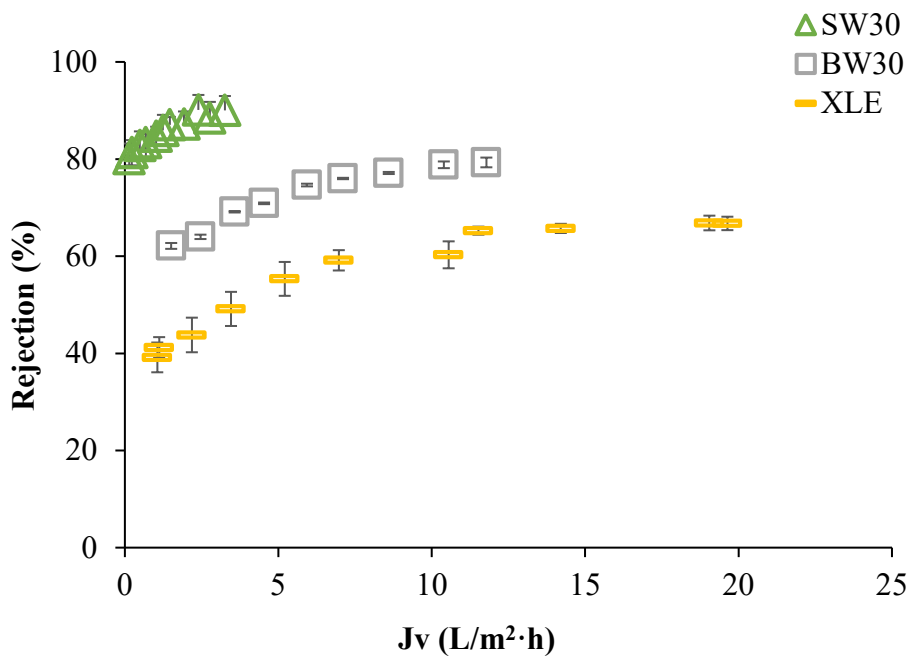
a)
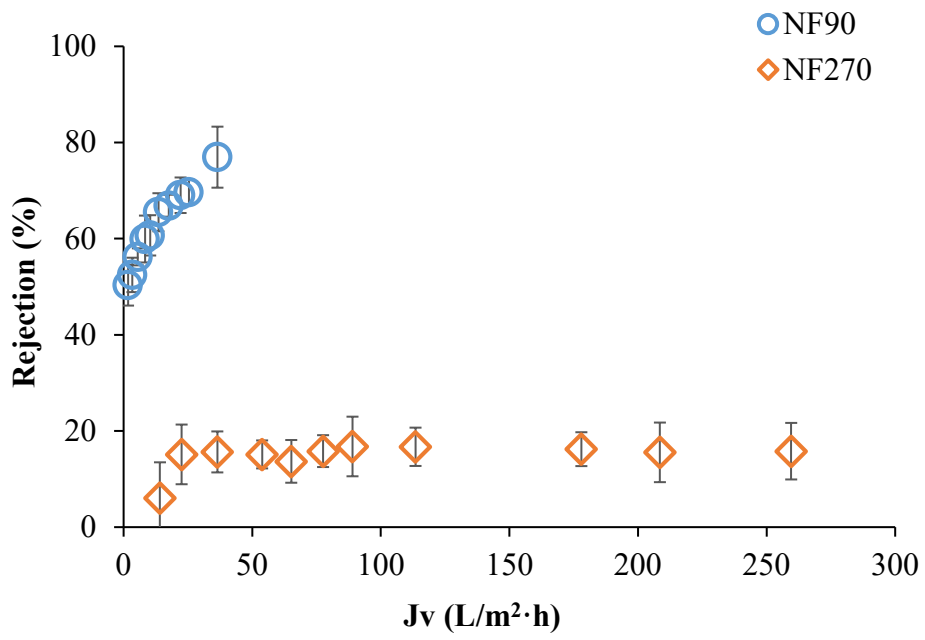
b)

Figure 2. Furfural rejection evolution with the trans-membrane flux by using a) NF (NF270 and NF90) and b) RO membranes (XLE, BW30 and SW30), respectively.

In regard with furfural rejection, NF membranes showed different behavior between them, whereas the performance of RO membranes was similar. As it can be seen in **Figure 2a**, the furfural rejection by NF270 was 16±6%, whereas 77±6% was obtained using NF90, at 20 bar. Then, it can be said that the passage of furfural into the permeate side of the NF membrane was around 84% and 23%, respectively. On the other hand, the three RO tested membranes showed (at 20 bar) furfural rejections between 67±2% to 90±3% as exhibited in **Figure 2b**. In this sense, NF90 and RO membranes (XLE, BW30 and SW30) presented the same behavior, e.g. higher furfural rejections, in comparison with NF270 membrane. This performance could be possible due to their membrane composition, since NF270 is composed by semi-aromatic TFC, whereas NF90 and RO membranes are formed by fully aromatic TFC (see **Table 1**). In fact, Nguyen et al. [39] presented the NF90 membrane as RO membrane group for the detoxification of lignocellulosic hydrolysates on flat-sheet configuration set-up.

Table 2 summarises the published rejection results when treating furfural solutions by the NF and RO membranes studied (NF270, NF90, XLE, BW30 and SW30) in this work.

Furfural recovery with NF and RO membranes has not been widely studied, although it is a current topic, since it has been studied by some authors from 2011 to 2016 [34–39]. For this reason, most of the already published studies used model solutions to carry out the experiments in a flat-sheet configuration at lab-scale as well as in this work. **Table 2** takes into account several operational parameters, such as the initial furfural concentration, the initial pH of the feed solution, the membrane configuration or the TMP and on the other hand the furfural rejection obtained in each work.

Table 2. Bibliographic comparison for furfural rejections using NF (NF270 and NF90) and RO membranes (XLE, BW30 and SW30).

MEMBRANE	MODULE CONFIGURATION	FEED SOLUTION	INITIAL pH	INITIAL FURFURAL CONCENTRATION (g/L)	TMP (bar)	FURFURAL REJECTION (%)	REFERENCE
NF270	Flat-sheet	25 g/L xylose, 10 g/Lglucose and 4 g/L furfural	$\approx$ 3.8	4.0	$\approx$ 8.0	$\approx$ 1 .0	34
			3.0		5.0 to 11.0	-5.0 to 5.0	
	Flat-sheet	10 g/L xylose, 2 g/L glucose and 7.5 g/L furfural	3.0	7.5	35.0	-10.3	34
		10 g/L xylose, 18 g/L glucose and 7.5 g/L furfural				-3.5	
		40 g/L xylose, 2 g/L glucose and 7.5 g/L furfural				1.6	
		40 g/L xylose, 18 g/L glucose and 7.5 g/L furfural				-1.1	
	Flat-sheet	7.5 g/L xylose, 9 g/L glucose and 1 g/L furfural	3.0	1.0	4.0 to 20.0	$\approx$ 15.0 to 20.0	38
	Spiral-wound	15g/L xylose, 10 g/L glucose, 5 g/L arabinose, 5 g/L acetic acid, 1 g/L hydroxymethyl furfural (HMF), 0.5 g/L furfural, 0.05 g/L vanillin	3.0	0.5	4.0 to 18.0	$\approx$ - 0.01 to 0.02	39
	Flat-sheet	15g/L xylose, 10 g/L glucose, 5 g/L arabinose, 5 g/L acetic acid, 1 g/L hydroxymethyl furfural (HMF), 0.5 g/L furfural, 0.05 g/L vanillin	3.0	0.5	5.0 to 30.0	$\approx$ 0.0 to 2.0	37
	Flat-sheet	9 g/L furfural in ethanol/water (1:99 v/v)	3.8 ± 0.6	9.3 ±0.1	1.4 ± 0.3 to 20.0 ± 0.1	6.0 ± 1.5 to 16.8 ± 1.3	This work
NF90	Flat-sheet	25 g/L xylose, 10 g/L glucose and 4 g/L furfural into deionized water + H$_2$SO$_4$	$\approx$ 3.7	4.0	$\approx$ 15.0	$\approx$ 40.0	34
	Flat-sheet	7.5 g/L xylose, 9 g/L glucose and 1 g/L furfural	3.0	1.0	4.0 to 20.0	$\approx$ 15.0 to 45.0	38
	Flat-sheet	Lignocellulosic hydrolysate	5.0	1.5	33.5	42.0	36
	Flat-sheet	15g/L xylose, 10 g/L glucose, 5 g/L arabinose, 5 g/L acetic acid, 1 g/L hydroxymethyl furfural (HMF), 0.5 g/L	3.0	0.5	5.0 to 30.0	$\approx$ 20.0 to 60.0	37

	Module	Feed					Reference
		furfural, 0.05 g/L vanillin					
	Flat-sheet	9 g/L furfural in ethanol/water (1:99 v/v)	3.7 ± 0.1	8.6 ± 0.1	2.1 ± 0.1 to 20.1 ± 0.1	50.3 ± 2.1 to 77.0 ± 3.2	This work
XLE	Flat-sheet	15g/L xylose, 10 g/L glucose, 5 g/L arabinose, 5 g/L acetic acid, 1 g/L hydroxymethyl furfural (HMF), 0.5 g/L furfural, 0.05 g/L vanillin	3.0	0.5	5.0 to 30.0	≈ 60.0 to 95.0	[37]
	Flat-sheet	9 g/L furfural in ethanol/water (1:99 v/v)	3.9 ± 0.1	9.1 ± 0.1	1.7 ± 0.1 to 20.0 ± 0.1	39.2 ± 3.1 to 66.8 ± 1.5	This work
BW30	Spiral-wound	0.18 g/L acetic acid, 0.14g/L butanoic acid, 0.23 g/L 2,3-butanediol, 0.02 g/L furfural, 0.02 g/L 2-phenethyl alcohol	7.0	0.02	5.0 to 30.0	≈ 5.0 to 65.0	[35]
	Flat-sheet	Lignocellulosic hydrolysate	5.0	1.5	40.4	92.0	[36]
	Flat-sheet	9 g/L furfural in ethanol/water (1:99 v/v)	3.5 ± 0.1	8.5 ± 0.1	4.1 ± 0.1 to 20.1 ± 0.1	62.1 ± 0.6 to 79.3 ± 1.0	This work
SW30	Flat-sheet	Lignocellulosic hydrolysate	5.0	1.5	40.4	99.0	[36]
	Flat-sheet	9 g/L furfural in ethanol/water (1:99 v/v)	3.6 ± 0.1	8.3 ± 0.1	1.5 ± 0.1 to 20.1 ± 0.1	80.1 ± 3.1 to 90.1 ± 3.0	This work

Comparing the NF membranes results, it can be concluded that NF270 allowed furfural passage into permeate, since its rejection varies from -10 to 20% depending on the feed and operation conditions used. For NF270 membrane, Nguyen et al. [39] used an spiral-wound membrane configuration in comparison with the other reported studies in **Table 2**, however, its furfural rejection results were comparable with those obtained when using a flat-sheet configuration. This behaviour was previously detected by Reig et al. [56] when comparing a salt mixture rejection using NF270 membrane in flat-sheet and spiral-wound configuration, concluding that its rejection was not affected by the membrane configuration. On the other hand, NF90 showed higher furfural rejections than N270 achieving furfural rejection values from 15 to 77%, being the highest the ones obtained in this work.

Moreover, comparing RO results showed in **Table 2** when using XLE and SW30 membranes, it was observed that furfural rejection depends on its initial concentration and operational TMP, obtaining higher rejections at higher TMPs and lower furfural feed concentrations. For instance, using XLE membrane, Nguyen et al. [37] reached higher concentration values (from 60 to 95%) than the ones obtained in this work (from 40 to 70%) working with lower furfural concentration and a higher TMP range. Using SW30 membrane, Gautam et al. [36] reached 99% of furfural rejection working around 40 bar and 1.5 g/L of feed furfural concentration, whereas in this work a maximum rejection of 90% was obtained working at 20 bar and initial furfural concentration around 9 g/L. Finally, comparing BW30 results, the same conclusion can be postulated, although it seems that the membrane configuration or the pH affects the furfural rejection, since Fargues et al. [35] obtained a lower furfural rejection working in a spiral-wound configuration and at higher pH (pH=7) than in this work (pH=3.5), where flat-sheet configuration was used.

Therefore, in this work it is remarkable that NF270 membrane could be used for furfural separation from lignocellulosic hydrolysates streams as a purification step, whereas NF90 and RO membranes (XLE, BW30 and SW30) could be employed as a furfural concentration step. Furthermore, other authors had reported conclusions when working with NF and RO membranes for furfural recovery. For example, Malmali et al. [57] studied the use of commercialize membrane including NF270, NF90, and RO99 for rejection of several compounds such as furfural, acetic acid, HMF, glucose, and xylose from synthetic biomass hydrolysate. They found out that inhibitory compounds consisting of furfural, HMF, and acetic acid were removed in the permeate. They also concluded that rejection levels of these compounds depend on several factors, such as membrane properties, feed properties, and operating conditions. Moreover, a study on the effect of different types of membranes towards furfural and HMF removal has been done recently by Wang et al. [58]. Commercial membranes consisting of two NF membranes (Desal-5 DK and Alfa Laval-NF) and two RO membranes (RO98pHt and RO99) were employed to separate these compounds (furfural and HMF) from model hydrolysate solutions and they observed that RO membranes were more efficient compared with the tested NF membranes for furfural removal.

3.3. Membrane characterization before and after furfural recovery

Table 3 shows the elemental compositions obtained by XPS. Elemental percentages exclude hydrogen since hydrogen is not quantifiable by this technique. The XPS results describe the near-surface region of the aromatic polyamide (PA) active layer for uncoated membranes, while for coated membranes is a combination of the near-surface regions of the coating and the PA active layer [59].

Table 3. Elemental composition obtained by XPS for each NF and RO membranes used before and after furfural recovery.

Type of membrane		C (%)	N (%)	O (%)	Minor elements (%)
NF	NF270 virgin	72.7	10.3	15.6	1.4
	NF270 used	55.6	5.2	35.7	3.5
	NF90 virgin	75.9	11.0	12.9	0.2
	NF90 used	70.9	9.7	18.5	1.0
RO	XLE virgin	77.3	10.0	12.1	0.5
	XLE used	67.0	8.4	23.1	1.5
	BW30 virgin	75.3	10.3	13.9	0.5
	BW30 used	72.0	8.5	19.2	0.2
	SW30 virgin	76.1	1.1	22.2	0.6
	SW30 used	73.2	6.0	20.4	0.3

The NF and RO virgin membranes were composed between 72.7-77.3% of C, 1.1-11.0% of N and 12.1-22.2% of O as exhibited in **Table 3**. The elemental composition for all membranes tested was similar, however it is remarkable that N and O amount in SW30 virgin membrane was different, since it had the smallest percentage of N and the highest percentage of O. This composition is in agreement with other works [59].

Additionally, N, C and O variation from the virgin coated membranes (BW30 and SW30) to the used ones was lower than for the uncoated membranes (NF270, NF90 and XLE). Thus, coated membranes exhibited a more stable behaviour, in terms of elemental composition, than uncoated membranes due to their coating layer.

In regard to furfural filtration process, NF and RO membranes showed a decrease on C and N content, whereas the O amount increased slightly. Finally, the membrane, which suffered the biggest change in terms of elemental composition, between the virgin and the used membranes, was the NF270.
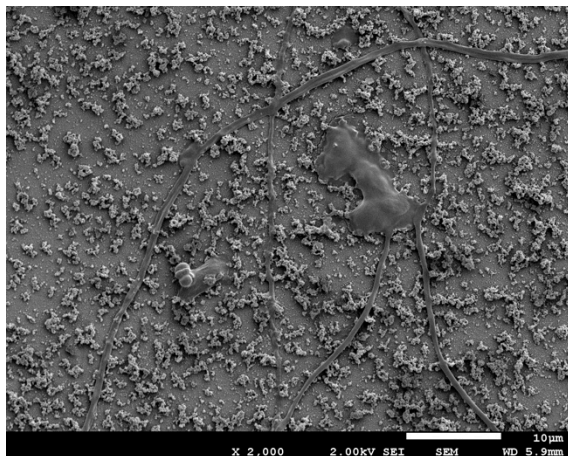
On the other hand, **Figure 3** exhibited the surface morphology of each virgin NF and RO membranes and each membrane after furfural filtration process.
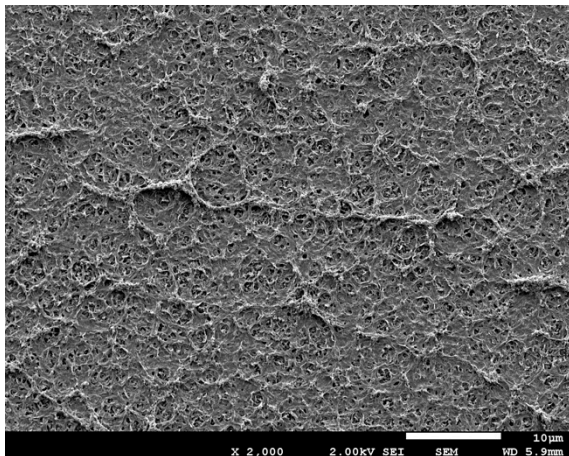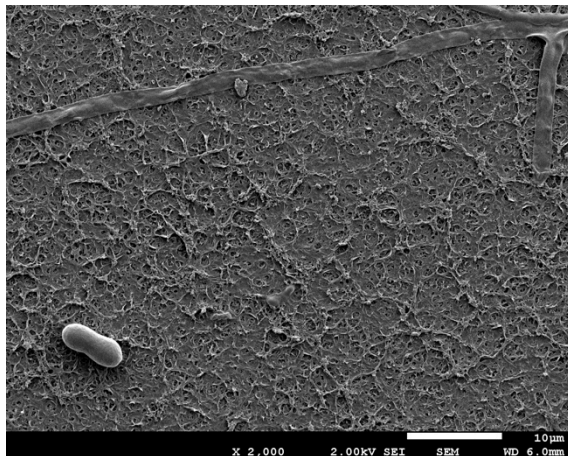
a)

NF270 virgin
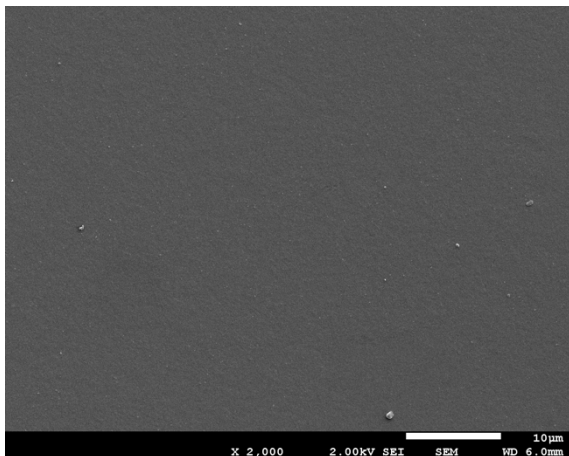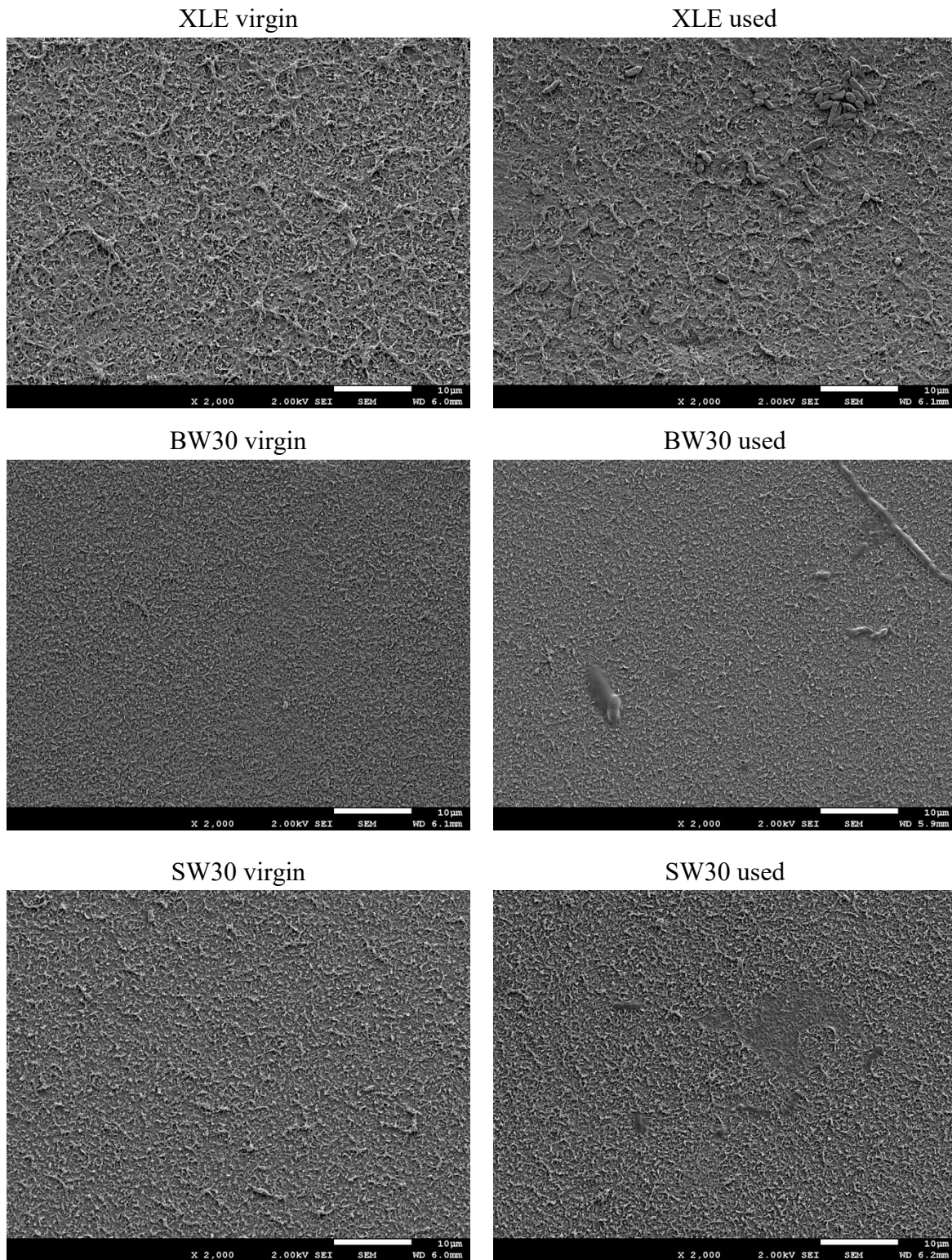
NF270 used

NF90 virgin

NF90 used

b)

XLE virgin   XLE used

BW30 virgin   BW30 used

SW30 virgin   SW30 used

Figure 3. SEM images for virgin (left) and used (right) a) NF and b) RO membranes**.**

20

As it can be seen, SEM images for NF90 and RO (XLE, BW30 and SW30) virgin and used membranes were similar, indicating that neither fouling occurred nor elements were stacked in the membrane surface during the high-concentrated furfural filtration tests. However, membrane surface images for NF270 membrane before and after use indicated changes during the performances. As mentioned previously, linearity of permeate flux and TMP indicates that membrane fouling and compaction effects are negligible [34], however as it was seen in **Figure 1**, the lower regression coefficient (0.912) was obtained by NF270. Therefore, it can be said that fouling occurred during the furfural recovering by NF270, as was also corroborated by the differences between the SEM images of raw and used NF270 membrane (**Figure 3)**, whereas it was not seen for the other membranes tested in this work.

4. CONCLUSIONS

It was observed that nanofiltration (using NF270 and NF90 membranes) and reverse osmosis (by XLE, BW30 and SW30 membranes) processes could be used for furfural recovery from mimicking oil palm hydrolysate streams. Additionally, it is necessary to remark that the furfural concentration used in these assays (9 g/L) is the highest tested in the literature with the mentioned type of membranes. Results indicated that NF membranes provided higher trans-membrane flux (around 260 and 37 $L/m^2 \cdot h$ using NF270 and NF90 membranes, respectively) than RO membranes (about 19, 12 and 3 $L/m^2 \cdot h$ for XLE, BW30 and SW30, respectively) working at 20 bar. Moreover, higher furfural rejections (67%-90%) were observed by means of NF90 and RO membranes in comparison with NF270 (16%) at 20 bar in flat-sheet configuration. Overall, furfural could be purified from lignocellulosic hydrolysates by using NF270 since high furfural passage into permeate was achieved, while furfural could be concentrated by NF90 and RO membranes due to its high rejection values obtained.

ACKNOWLEDGMENTS

REFERENCES

1   Naik SN, Goud V V., Rout PK, Dalai AK. Production of first and second generation biofuels: A comprehensive review. *Renew Sustain Energy Rev* 2010; **14**: 578–597.

2   Machado G, Leon S, Santos F, Lourega R, Dullius J, Mollmann ME *et al.* Literature Review on Furfural Production from Lignocellulosic Biomass. *Nat Resour* 2016; **07**: 115–129.

3   Dias AA, Freitas GS, Marques GSM, Sampaio A, Fraga IS, Rodrigues MAM *et al.* Enzymatic saccharification of biologically pre-treated wheat straw with white-rot fungi. *Bioresour Technol* 2010; **101**: 6045–6050.

4   Dussan K, Girisuta B, Haverty D, Leahy JJ, Hayes MHB. Kinetics of levulinic acid and furfural production from Miscanthus×giganteus. *Bioresour Technol* 2013; **149**: 216–224.

5   Ji H, Chen L, Zhu JY, Gleisner R, Zhang X. Reaction Kinetics Based Optimization of Furfural Production from Corncob Using a Fully Recyclable Solid Acid. *Ind Eng Chem Res* 2016; **55**: 11253–11259.

6   Peleteiro S, da Costa Lopes AM, Garrote G, Bogel-Łukasik R, Parajó JC. Manufacture of furfural in biphasic media made up of an ionic liquid and a co-solvent. *Ind Crops Prod* 2015; **77**: 163–166.

7   Sweygers N, Dewil R, Appels L. Production of Levulinic Acid and Furfural by Microwave-Assisted Hydrolysis from Model Compounds: Effect of Temperature, Acid

Concentration and Reaction Time. *Waste and Biomass Valorization* 2018; **9**: 343–355.

8   Antal MJ, Leesomboon T, Mok WS, Richards GN. Mechanism of formation of 2-furaldehyde from d-xylose. *Carbohydr Res* 1991; **217**: 71–85.

9   Nimlos MR, Qian X, Davis M, Himmel ME, Johnson DK. Energetics of Xylose Decomposition as Determined Using Quantum Mechanics Modeling - The Journal of Physical Chemistry A (ACS Publications). *J Phys Chem A* 2006; **110**: 11824–11838.

10   Mamman AS, Lee J-M, Kim Y-C, Hwang IT, Park N-J, Hwang YK *et al.* Furfural: Hemicellulose/xylose- derived biochemical. *Biofuels, Bioprod Biorefining* 2008; **2**: 438–454.

11   Mazar A, Jemaa N, Wafa Al Dajani W, Marinova M, Perrier M. Furfural production from a pre-hydrolysate generated using aspen and maple chips. *Biomass and Bioenergy* 2017; **104**: 8–16.

12   Mariscal R, Maireles-Torres P, Ojeda M, Sádaba I, López Granados M. Furfural: A renewable and versatile platform molecule for the synthesis of chemicals and fuels. *Energy Environ Sci* 2016; **9**: 1144–1189.

13   Baktash MM, Ahsan L, Ni Y. Production of furfural from an industrial pre-hydrolysis liquor. *Sep Purif Technol* 2015; **149**: 407–412.

14   Chheda JN, Dumesic JA. An overview of dehydration, aldol-condensation and hydrogenation processes for production of liquid alkanes from biomass-derived carbohydrates. *Catal Today* 2007; **123**: 59–70.

15   Xing R, Qi W, Huber GW. Production of furfural and carboxylic acids from waste aqueous hemicellulose solutions from the pulp and paper and cellulosic ethanol industries. *Energy Environ Sci* 2011; **4**: 2193–2205.

16   Gilkey MJ, Panagiotopoulou P, Mironenko A V., Jenness GR, Vlachos DG, Xu B. Mechanistic Insights into Metal Lewis Acid-Mediated Catalytic Transfer Hydrogenation of Furfural to 2-Methylfuran. *ACS Catal* 2015; **5**: 3988–3994.

17   Dutta S, De S, Saha B, Alam MI. Advances in conversion of hemicellulosic biomass to furfural and upgrading to biofuels. *Catal Sci Technol* 2012; **2**: 2025–2036.

18   Srivastava S, Jadeja GC, Parikh J. A versatile bi-metallic copper-cobalt catalyst for liquid phase hydrogenation of furfural to 2-methylfuran. *RSC Adv* 2016; **6**: 1649–1658.

19   Bui L, Luo H, Gunther WR, Román-Leshkov Y. Domino reaction catalyzed by zeolites with Brønsted and Lewis acid sites for the production of γ-valerolactone from furfural. *Angew Chemie - Int Ed* 2013; **52**: 8022–8025.

20   Tukacs JM, Bohus M, Dibó G, Mika LT. Ruthenium-catalyzed solvent-free conversion of furfural to furfuryl alcohol. *RSC Adv* 2017; **7**: 3331–3335.

21   Alonso-Fagúndez N, Agirrezabal-Telleria I, Arias PL, Fierro JLG, Mariscal R, Granados ML. Aqueous-phase catalytic oxidation of furfural with H2O2: High yield of maleic acid by using titanium silicalite-1. *RSC Adv* 2014; **4**: 54960–54972.

22   Yang Y, Ma J, Jia X, Du Z, Duan Y, Xu J. Aqueous phase hydrogenation of furfural to tetrahydrofurfuryl alcohol on alkaline earth metal modified Ni/Al2O3. *RSC Adv* 2016; **6**: 51221–51228.

23   Wu WP, Xu YJ, Chang SW, Deng J, Fu Y. pH-Regulated Aqueous Catalytic Hydrogenation of Biomass Carbohydrate Derivatives by Using Semisandwich Iridium Complexes. *ChemCatChem* 2016; **8**: 3375–3380.

24   Wang T, Li K, Liu Q, Zhang Q, Qiu S, Long J *et al.* Aviation fuel synthesis by catalytic conversion of biomass hydrolysate in aqueous phase. *Appl Energy* 2014; **136**: 775–780.

25   Chan YH, Yusup S, Quitain AT, Uemura Y, Sasaki M. Bio-oil production from oil palm biomass via subcritical and supercritical hydrothermal liquefaction. *J Supercrit Fluids* 2014; **95**: 407–412.

26   Minami E, Saka S. Decomposition behavior of woody biomass in water-added supercritical methanol. *J Wood Sci* 2005; **51**: 395–400.

27   Mohamad N, Mohamad Yusof NN, Yong TLK. Furfural production under subcritical

alcohol conditions: Effect of reaction temperature, time, and types of alcohol. *J Japan Inst Energy* 2017; **96**: 279–284.

28   Teella A, Huber GW, Ford DM. Separation of acetic acid from the aqueous fraction of fast pyrolysis bio-oils using nanofiltration and reverse osmosis membranes. *J Memb Sci* 2011; **378**: 495–502.

29   Reig M, Casas S, Valderrama C, Gibert O, Cortina JL. Integration of monopolar and bipolar electrodialysis for valorization of seawater reverse osmosis desalination brines : Production of strong acid and base. *Desalination* 2016; **398**: 87–97.

30   Reig M, Vecino X, Valderrama C, Gibert O, Cortina JL. Application of selectrodialysis for the removal of As from metallurgical process waters: Recovery of Cu and Zn. *Sep Purif Technol* 2018; **195**: 404–412.

31   Kaur I, Ni Y. A process to produce furfural and acetic acid from pre-hydrolysis liquor of kraft based dissolving pulp process. *Sep Purif Technol* 2015; **146**: 121–126.

32   Afonso MD. Assessment of NF and RO for the potential concentration of acetic acid and furfural from the condensate of eucalyptus spent sulphite liquor. *Sep Purif Technol* 2012; **99**: 86–90.

33   Xie Y, Liu S. Purification and concentration of paulownia hot water wood extracts with nanofiltration. *Sep Purif Technol* 2015; **156**: 848–855.

34   Qi B, Luo J, Chen X, Hang X, Wan Y. Separation of furfural from monosaccharides by nanofiltration. *Bioresour Technol* 2011; **102**: 7111–7118.

35   Fargues C, Sagne C, Szymczyk A, Fievet P, Lameloise ML. Adsorption of small organic solutes from beet distillery condensates on reverse-osmosis membranes: Consequences on the process performances. *J Memb Sci* 2013; **446**: 132–144.

36   Gautam AK, Menkhaus TJ. Performance evaluation and fouling analysis for reverse osmosis and nanofiltration membranes during processing of lignocellulosic biomass hydrolysate. *J Memb Sci* 2014; **451**: 252–265.

37   Nguyen N, Fargues C, Guiga W, Lameloise ML. Assessing nanofiltration and reverse osmosis for the detoxification of lignocellulosic hydrolysates. *J Memb Sci* 2015; **487**: 40–50.

38   dos Santos JLC, Fernandes MC, Lourenço PML, Duarte LC, Carvalheiro F, Crespo JG. Removal of inhibitory compounds from olive stone auto-hydrolysis liquors by nanofiltration. *Desalin Water Treat* 2011; **27**: 90–96.

39   Nguyen DTNN, Lameloise ML, Guiga W, Lewandowski R, Bouix M, Fargues C. Optimization and modeling of diananofiltration process for the detoxification of ligno-cellulosic hydrolysates - Study at pre-industrial scale. *J Memb Sci* 2016; **512**: 111–121.

40   Sagehashi M, Nomura T, Shishido H, Sakoda A. Separation of phenols and furfural by pervaporation and reverse osmosis membranes from biomass - superheated steam pyrolysis-derived aqueous solution. *Bioresour Technol* 2007; **98**: 2018–2026.

41   Lee JW, Trinh LTP, Lee HJ. Removal of inhibitors from a hydrolysate of lignocellulosic biomass using electrodialysis. *Sep Purif Technol* 2014; **122**: 242–247.

42   Reig M, Licon E, Gibert O, Yaroshchuk A, Cortina JL. Rejection of ammonium and nitrate from sodium chloride solutions by nanofiltration: Effect of dominant-salt concentration on the trace-ion rejection. *Chem Eng J* 2016; **303**: 401–408.

43   Pagès N, Reig M, Gibert O, Cortina JL. Trace ions rejection tunning in NF by selecting solution composition: Ion permeances estimation. *Chem Eng J* 2017; **308**. doi:10.1016/j.cej.2016.09.037.

44   DOW FILMTEC^{TM} NF270-4040. 2018.https://www.dow.com/en-us/markets-and-solutions/products/DOWFILMTECNanofiltration4Elements/DOWFILMTECNF2704040 (accessed 1 Oct2018).

45   DOW FILMTEC^{TM} NF90-4040. 2018.https://www.dow.com/en-us/markets-and-solutions/products/DOWFILMTECNanofiltration4Elements/DOWFILMTECNF904040 (accessed 1 Oct2018).

46   DOW FILMTEC^{TM} XLE-4040. 2018.https://www.dow.com/en-us/markets-and-

solutions/products/DOWFILMTECBrackishWaterReverseOsmosis4Elements/DOWFILM
TECXLE4040 (accessed 1 Oct2018).

47   DOW FILMTEC^{TM} BW30-4040. 2018.https://www.dow.com/en-us/markets-and-
solutions/products/DOWFILMTECBrackishWaterReverseOsmosis4Elements/DOWFILM
TECBW304040 (accessed 1 Oct2018).

48   DOW FILMTEC^{TM} SW30-4040. 2018.https://www.dow.com/en-us/markets-and-
solutions/products/DOWFILMTECSeawaterReverseOsmosis4Elements/DOWFILMTECS
W304040 (accessed 1 Oct2018).

49   Chuyang Y. Tang, Young-Nam Kwon JOL. Effect of membrane chemistry and coating
layer on physiochemical properties of thin film composite polyamide RO and NF
membranes II. Membrane physiochemical properties and their dependence on polyamide
and coating layers. *Desalination* 2009; **242**: 168–182.

50   Carrión-Prieto P, Martín-Ramos P, Hernández-Navarro S, Sánchez-Sastre LF, Marcos-
Robles JL, Martín-Gil J. Furfural, 5-HMF, acid-soluble lignin and sugar contents in C.
ladanifer and E. arborea lignocellulosic biomass hydrolysates obtained from microwave-
assisted treatments in different solvents. *Biomass and Bioenergy* 2018; **119**: 135–143.

51   Chi C, Zhang Z, Chang HM, Jameel H. Determination of furfural and
hydroxymethylfurfural formed from biomass under acidic conditions. *J Wood Chem
Technol* 2009; **29**: 265–276.

52   MWCO NF membranes DOW.
2018.https://dowac.custhelp.com/app/answers/detail/a_id/4925/~/filmtec-membranes---
nanofiltration---mwco (accessed 17 Dec2018).

53   Ates N, Uzal N. Removal of heavy metals from aluminum anodic oxidation wastewaters
by membrane filtration. *Environ Sci Pollut Res* 2018; **25**: 22259–22272.

54   Teow YH, Ghani MSH, Hamdan WNAWM, Rosnan NA, Mazuki NIM, Ho KC.
Application of Membrane Technology towards The Reusability of Lake Water, Mine
Water, and Tube Well Water. *J Kejuruter* 2017; **29**: 131–137.

55   Drewes JE, Xu P, Bellona C, Amy G, Kim T, Adam M *et al.* Rejection of emerging organic micropollutants in nanofiltration/revserse osmosis memrbane applications. *Water Environ Res* 2005; **77**: 40–48.

56   Reig M, Pagès N, Licon E, Valderrama C, Gibert O, Yaroshchuk A *et al.* Evolution of electrolyte mixtures rejection behaviour using nanofiltration membranes under spiral wound and flat-sheet configurations. *Desalin Water Treat* 2014; **56**: 3519–3529.

57   Malmali M, Stickel JJ, Wickramasinghe SR. Sugar concentration and detoxification of clarified biomass hydrolysate by nanofiltration. *Sep Purif Technol* 2014; **132**: 655–665.

58   Wang T, Meng Y, Qin Y, Feng W, Wang C. Removal of furfural and HMF from monosaccharides by nanofiltration and reverse osmosis membranes. *J Energy Inst* 2018; **91**: 473–480.

59   Coronell O, Mariñas BJ, Cahill DG. Depth heterogeneity of fully aromatic polyamide active layers in reverse osmosis and nanofiltration membranes. *Environ Sci Technol* 2011; **45**: 4513–4520.